Automatic Identification of Large-Scale Field-Aligned Current Structures and its Application to Night-Side Current Systems

T. Higuchi
The Institute of Statistical Mathematics, Tokyo, Japan

S. Ohtani
The Johns Hopkins University Applied Physics Laboratory, Laurel, Maryland, U.S.A.

The present paper reports a newly developed procedure to automatically identify a spatial structure of large-scale field-aligned currents (FACs) from satellite magnetic field measurements. The procedure is based on the concept of the first-order B-spline fitting with variable (i.e., movable) node positions, which may be envisioned as fitting line segments to a plot of a magnetic field component. The number of node points is optimized for each current sheet crossing so that a certain information criterion is minimized. The properties of a FAC system such as its location and intensity can be easily calculated from the information of node points. The procedure is applied to the entire set of nightside magnetic field measurements (1339 days) made by the DMSP-F7 satellite and for demonstration, the intensity of nightside region-1 FACs is examined as a function of magnetic latitude. The results not only confirm the general expectation that intense region 1 currents tend to be observed at lower latitudes but also quantify the relationship between the current intensity and latitude. The capability of such quantification should be useful for future studies including practical applications such as space weather forecast.

1. INTRODUCTION

The importance of FACs in the electromagnetic coupling between the magnetosphere and ionosphere cannot be overstated. The characteristics of FACs have been examined for more than three decades since FACs were initially detected by a low-altitude satellite at the very early stage of satellite observation [e.g., *Zmuda et al.*, 1966; *Cummings and Dessler*, 1967]. Large-scale FACs are classified into three systems, that is, region 2 (R2), region 1 (R1), and region 0 (R0) systems from equatorward to poleward [*Iijima and Potemra*, 1976]. The R0 system is distributed in the midday sector, whereas the R2 and R1 currents encircle a magnetic pole but are off-centered toward midnight. The R1 FAC tends to flow toward and away from the ionosphere in the morning and evening sectors, respectively, and at a given local time the polarity of a R2 current is the opposite to that of a R1 current.

Although such average properties of large-scale FACs are well accepted, it is also known that the spatial structure and intensity of these current systems are far from stationary and depend on both external and internal conditions. However, since the analysis of FACs has been

Magnetospheric Current Systems
Geophysical Monograph 118

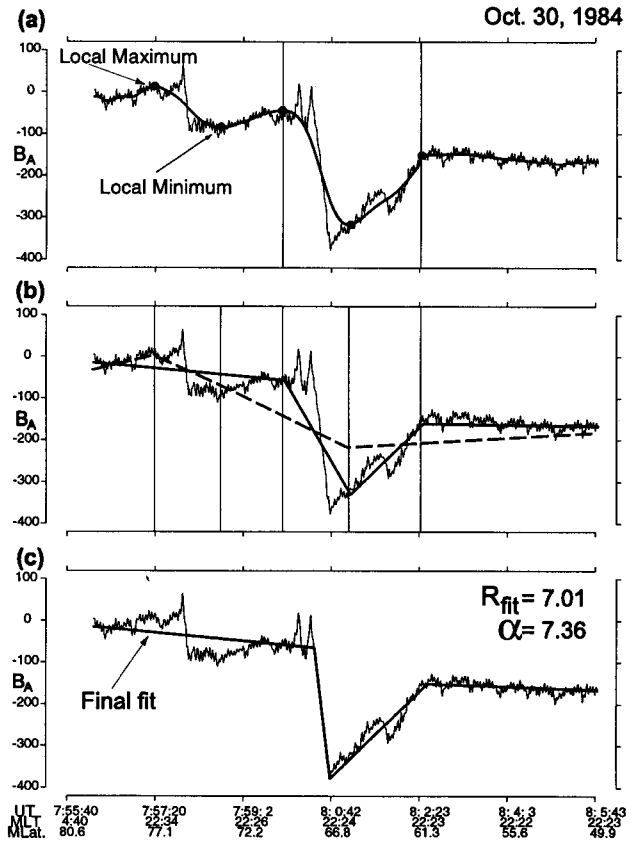

Figure 1. Application of the procedure to the DMSP-F7 data of October 30, 1984. (a) Determination of node-point candidates (local minima and maxima) based on the smoothed data. (b) Search for the optimum combination of node points. (c) The final adjustment based on the original data.

strongly depending on visual inspection of satellite magnetic field data, a large statistical study not only requires significant effort but also tends to lack quantification. Considering that the archive of satellite data keeps growing, we believe that a computational procedure to identify large-scale FACs is most needed for performing a data analysis of the next level, which eventually will provide better understanding of the electrodynamic processes of the magnetosphere. In the following we explain a procedure we developed for this purpose and present the results of an initial application to nightside current systems.

2. AUTOMATIC IDENTIFICATION OF LARGE-SCALE FAC

In this section we briefly explain the scheme we developed to automatically identify the spatial structure of large-scale FACs from satellite magnetic field data. Measurements of two magnetic field components transverse to the background magnetic field are used for this procedure. We assume that a data file to be processed includes a single crossing of a FAC region. The procedure consists of three tasks, that is, the determination of the interval of a FAC crossing, the rotation of magnetic field vectors to the direction of the maximum variance, and fitting of line segments to an (imaginary) plot of that component [*Hiragi et al.*, 1985; *Kitagawa and Higuchi*, 1998]. Each task consists of a few steps, which are explained in the following:

Step 1: An interval of a FAC crossing is preparatorily determined from parameterized characteristics such as variances of magnetic field variations. Only the east–west magnetic component is used at this step.

Step 2: The principal component analysis (PCA) (also known as the minimum variance analysis) is applied to magnetic field measurements during a FAC crossing. The maximum-to-minimum ratio of two eigenvalues, α, represents the extent to which the spatial structure of FACs can be approximated by an extending sheet. Measured magnetic vectors are rotated, and only the component in the maximum variance direction, which is usually close to the azimuthal direction, is used in the subsequent procedure. We refer to this component as B_A.

(Note: Step 1 is necessary before Step 2 because if the PCA is applied to the whole crossing, a gradual background variation affects the result of Step 2. Such a variation is attributed partly to differences between actual magnetic field and model magnetic field subtracted and partly to a smearing effect of FACs.)

Step 3: The interval of a FAC crossing is redefined based on the maximum-variance component.

Step 4: A smoothing filter [*Higuchi*, 1991] is constructed by examining the autocorrelation of magnetic variations for each of the three intervals, that is, intervals equatorward, inside, and poleward of the FAC crossing. After smoothing the data with the constructed filters, all local maximum and minimum points plus two points at both edges of the FAC crossing are registered as candidates for the boundaries of FAC sheets; these points are called node points. Figure 1a shows a plot of B_A (thin line), as an example, for a DMSP-F7 nightside pass of October 30, 1984. The two vertical lines indicate the poleward and equatorward edges of the FAC crossing, which were determined at Step 3. The thick line plots the smoothed data. The solid circles indicate the node points.

Step 5: For an assumed number of FAC sheets (the optimum number of FAC sheets will be determined at the next step), all possible combinations of node points are

selected. For a two-sheet structure, for example, three node points are required to fit segments to the plot: two points at the beginning and end of the FAC region and another point at the interface between the two systems. If there are five node points, we have 10 (= $_5C_3$) such combinations. The goodness of each combination is evaluated by the residual sum of squares (RSS) between measurements and segments connecting the selected node points. The combination with the minimum RSS is registered as the optimum one for each number of FAC sheets. For the example shown in Figure 1b, the fit by the thick line segments approximates the actual data much better than the fit by the broken line segments, giving a smaller RSS; the former actually provides the best fit for this number of FAC sheets and the best fit overall.

Step 6: An information criterion called Akaike Information Criterion (AIC) [*Akaike*, 1974; *Sakamoto et al.*, 1986] is introduced to determine the number of FAC sheets, J, which is expressed as

$$\mathrm{AIC}(J)=N\log\left(\frac{RSS(J)}{N}\right)+4J+Const.,$$

where N is the number of data points.

This parameter evaluates the efficiency of fitting in terms of the number of fitting parameters, J in the present case. RSS is a decreasing function with J; in other words, the measurements can be fitted better with more node points. Thus the value of RSS alone does not determine J. The number of FAC sheets is determined to be the one that minimizes AIC, and accordingly the optimum combination of node points is selected.

Step 7: The values of the smoothed data at local maxima or minima do not always agree with those of the original data. The procedure adopts the quasi-Newton method to make the fitted segments trace more closely to the original data. The thick line in Figure 1c shows the result of this refinement for the given example.

Step 8: The properties of each FAC sheet such as its location and intensity are calculated from the locations of node points and are registered. The goodness of the optimum fit, R_{fit}, is defined as the standard deviation for the optimum fit divided by the intensity of the most intense FAC and is also recorded. For a magnetic slope to be identified as a FAC sheet, (1) the magnitude of the associated magnetic change must be larger than both 50 [nT] and 30% of the magnitude of the magnetic change associated with the most intense FAC for each pass, and (2) the slope must be steeper than 1.2 [nT/s], which corresponds to a current density of 0.128 [μA/m^2], if the trajectory is perpendicular to a current sheet.

There are a few other techniques for calculating the spatial distribution of FACs. One popular example is the assimilative mapping of ionospheric electrodynamics (AMIE) technique [*Richmond and Kamide*, 1988]. Although the AMIE is most useful for examining the time development of the global FAC distribution, it requires magnetic field data from numerous ground stations, and it has to assume ionospheric conductance. A new technique reported by Weimer at the conference [*Weimer*, 1999] uses spherical harmonic functions for presenting the magnetic potential and does not require any assumption about the geometry of FACs. This technique, however, requires data assembled from many satellite passes to calculate the global distribution of FACs. In contrast with these techniques, the method we developed is basically the automation of the way we visually examine a plot of satellite magnetic field data. Because the method can be applied even to a single satellite pass, it may be easily implemented in a real-time processing of data. It can also be applied to an entire set of satellite data, allowing us to perform a large statistical study. The trade-off of our method is that it assumes the sheet structure of FACs, although the extent to which this assumption is justified is quantified by the principal component analysis. Thus, each technique has both pros and cons, and it is most important to choose the right one based on the purpose of a study.

3. APPLICATIONS

We have applied the procedure to the entire set of 1-s magnetometer data acquired by the DMSP-F7 satellite from December 1983 to January 1988 (1339 days). DMSP-F7 is a Sun-synchronous satellite with a nearly circular polar pass at about 835 km in altitude, with its ascending and descending nodes at 1030 and 2230 local time (LT), respectively. The orbital period is about 101 min. The satellite crossed the nightside auroral oval more than 35,000 times during its entire mission. After checking data gap and screening of crossings by the principal component analysis and the segment fitting (we use only crossings with $\alpha > 2$ and $R_{\mathrm{fit}} < 8$), the procedure identified the structure of FACs for 5,590 and 4,386 crossings in the northern and southern hemispheres, respectively. This task is doable with an ordinary PC machine, as demonstrated with a notebook PC at the conference. With a 260-MHz Pentium-II processor it takes less than 5 s to process one crossing or a minute to transact a 1-day data file.

Table 1 lists the number of crossings for each number of FAC sheets. Note that for each number of FAC sheets there are two distinct types in terms of the polarities (upward or downward) of FACs. Figure 2 shows an example of each

Table 1. Number of Passes for Different FAC Structures Crossed by DMSP-F7 on the Nightside

	Number of FAC sheets						
	1	2	3	4	5	6	Total
North	53	3,381	1,561	483	110	2	5,590
South	338	2,673	956	318	101	0	4,386

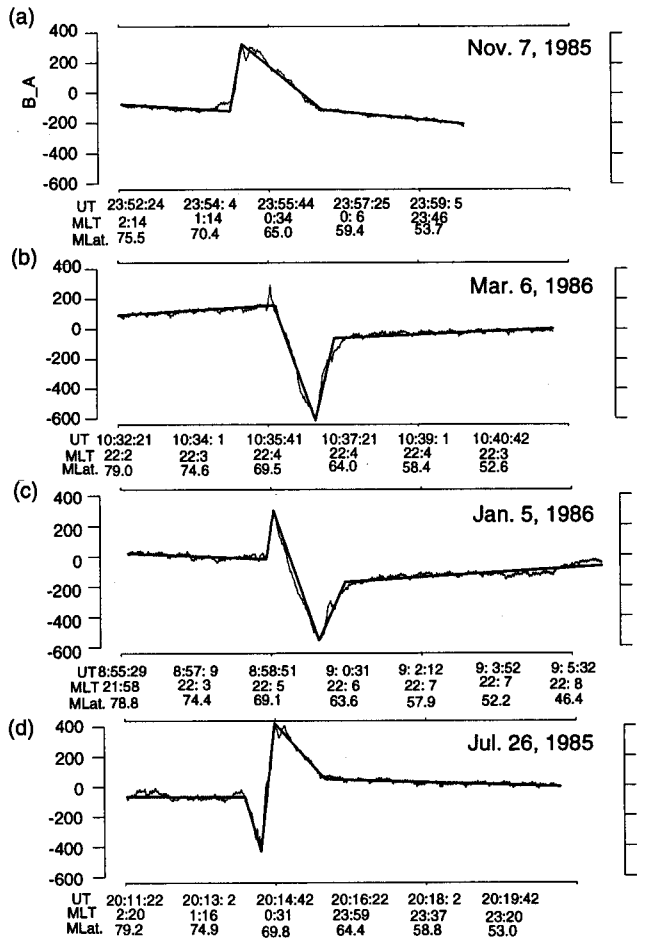

Figure 2. Examples of (a and b) two and (c and d) three field-aligned current sheet crossings. The result of the automatic procedure (thick line) is superposed on the plot of the original data (thin line).

type for two- and three-sheet structures. The result of the automatic procedure (thick line) is superposed on the actual measurement (thin line).

To demonstrate the potential of the developed procedure for studying FACs, we examine the relationship between the latitude and the intensity of nightside R1 FACs. We used data only from the northern hemisphere (the northern passes of DMSP-F7 cover both premidnight and postmidnight sectors, but the southern passes do not) and focused on downward-flowing R1 FACs observed as a part of a two- or three-sheet structure. Examples of such events are shown in Figures 2a and 2d. A pair of downward-flowing R1 and upward-flowing R2 currents should be accompanied by a westward-flowing electrojet in the ionosphere, which is an important element of the magnetospheric substorm. Here we note that the term "region 1" or "region 2" in a general sense without distinction in terms of their association with the substorm process.

Figure 3 plots the location of the center of region 1 FAC sheets in the frame of magnetic latitude (MLat) vs. magnetic local time (MLT) for a total of 2061 events. The solid circles represent two-sheet structure events with $\Delta B < 200$ nT (ΔB is the magnitude of a change in B_A throughout the R1 FAC sheet crossing), whereas the crosses and dots represent three-sheet structure events and other two-sheet structure events, respectively. The solid curve represents the optimum fit of a quadratic function for the solid-circled events, which is expressed as

$$\mathrm{MLat}(\Delta\mathrm{MLT}) = 68.94 - 0.1133 \times (\Delta\mathrm{MLT}) + 1.276 \times (\Delta\mathrm{MLT})^2$$

$$\Delta\mathrm{MLT} = \mathrm{MLT}\ (\text{for MLT} > 0) / \mathrm{MLT} - 24\ (\text{for MLT} < 24)$$

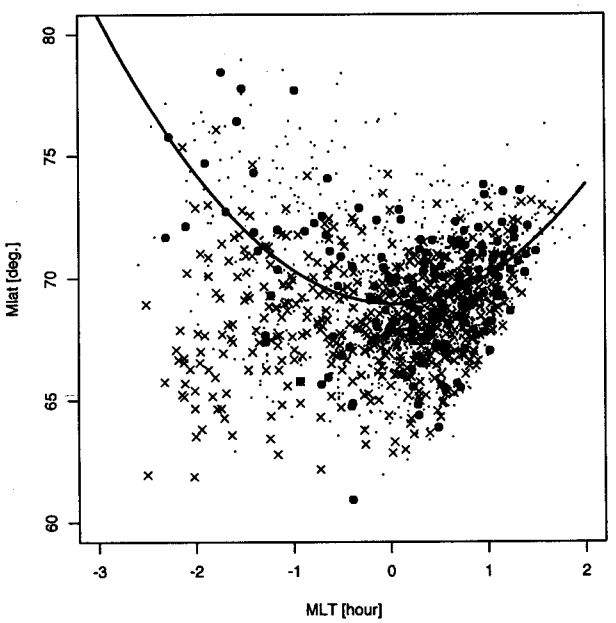

Figure 3. Positions of the center of R1 FAC sheet crossings in the MLat vs. MLT format for two-sheet structure events with $\Delta B < 200$ nT (solid circles), other two-sheet structure events (dots) and three-sheet structure events (crosses). The solid line represents the result of the quadratic fit for the solid circles.

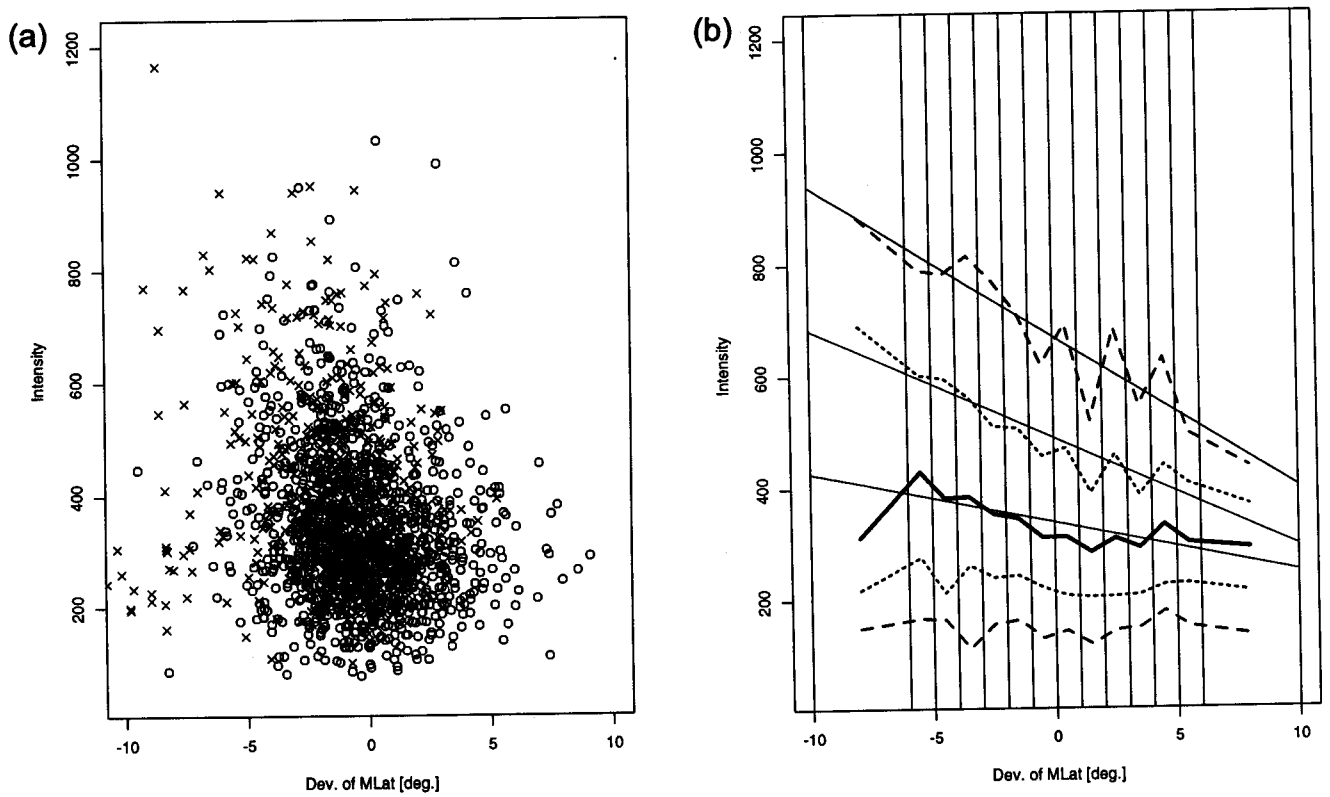

Figure 4. (a) The magnitude of magnetic perturbations (ΔB) associated with R1 currents plotted against ΔMLT for two-sheet (open circles) and three-sheet (crosses) structure events. (b) The values of ΔB at the medium, $\pm\sigma$, and $\pm 2\sigma$, along with the result of the linear fit for the medium, $+\sigma$, and $+2\sigma$ values.

We did the same fitting to events with $\Delta B < 300$ nT but found that the result is not very different. We use MLat(ΔMLT) as a reference and evaluate the latitude of a R1 FAC as a deviation from MLat(ΔMLT), which we denote as ΔMLat.

Figure 4a plots ΔB against ΔMLat. Again the crosses indicate events with three-sheet structure. Events with small values of ΔB are absent because we required $\Delta B > 50$ nT at Step 8 of our procedure. The data points scatter significantly. Nevertheless, it is clear that the lower bound of ΔB does not depend on ΔMLat, whereas the upper bound increases as ΔMLat decreases. This can be interpreted in the following way in terms of the substorm-associated dynamics. As the substorm growth phase proceeds, the auroral oval shifts equatorward [*Feldstein and Starkov*, 1967] and so does the R1 current. Although the intensity of such a R1 current may be as small as that found at higher latitude during quiet periods, the intensity of a R1 current after a substorm onset, even if located at the same latitude, can be significantly larger. The extent of the intensification is inferred to depend on the preonset energy storage, which is positively correlated with the size of the polar cap and therefore with the extent of the equatorward shift of the R1 current. The correlation between the intensity and latitude of the westward electrojet reported previously [*Kamide and Akasofu*, 1974] is consistent with this idea. It is also found that for larger negative values of ΔMLat, all intense R1 currents are a part of the three-sheet structure. By combining the fact that three-sheet structure events tend to take place in the premidnight sector (Figure 3), we infer that such intense R1 currents are related to the development of the Harang discontinuity.

The large number of events of our data set allows us to quantify the relationship of ΔB vs. ΔMLat. In Figure 4b ΔMLat is binned with a 1° increment from −6° to +6° leaving two bins outside of this range. For each bin, the values of ΔB at the medium, $\pm\sigma$, and $\pm 2\sigma$ are calculated based on the deduced likelihood and are connected by different lines. In contrast with the value at -2σ, which is almost constant irrespective of ΔMLat, the value at $+2\sigma$ increases with decreasing ΔMLat. The solid lines superposed on the plot for the medium, $+\sigma$, and $+2\sigma$

represent the result of the least-square fit and are expressed as

$$\Delta B(\text{medium}) = 338 - 8.9 \times \Delta\text{Mlat},$$

$$\Delta B(+\sigma) = 488 - 19.4 \times \Delta\text{Mlat},$$

$$\Delta B(+2\sigma) = 669 - 26.9 \times \Delta\text{MLat}.$$

ΔB at the DMSP altitude (835 km) can be mapped to the ionosphere (110 km) by multiplying a factor of 1.17 (= $[(1\ R_E + 835\ \text{km})/(1\ R_E + 110\ \text{km})]^{1.5}$). The current intensity corresponding to $\Delta B(+2\sigma)$, $J_{\text{FAC}}(+2\sigma)$ at the ionospheric altitude is given by

$$J_{\text{FAC}}(+2\sigma)\ [\text{mA/m}] = 0.8 \times \Delta B\ [\text{nT; at 110 km}]$$

$$= 0.93 \times \Delta B\ [\text{nT; at 865 km}]$$

$$= 623 - 25.0 \times \Delta\text{MLat}.$$

Provided that this current is closed with an upward-flowing FAC through a latitudinal Pedersen current and that the Hall conductivity is twice the Pedersen conductivity, the intensity of the westward electrojet, which we assume is mostly a Hall current, can be estimated by

$$J_{\text{Hall}}(+2\sigma)\ [\text{mA/m}] = 1246 - 50 \times \Delta\text{MLat}.$$

The above formula provides an estimate of the intensity of the most intense westward electrojet expected as a function of ΔMLat. The above formula, however, may overestimate the electrojet intensity, since, in the three-sheet structure, a part of the region 1 current is closed with a current poleward of the region 1 current.

4. SUMMARY AND FUTURE PROSPECTS

In this study we developed an automatic procedure to identify the structure of large-scale FAC systems from low-altitude satellite magnetic field measurements. We successfully applied the procedure to the DMSP-F7 magnetometer data and examined the relationship between the latitude and the intensity of the nightside R1 current. It is demonstrated that this procedure allows us to quantitatively examine a subject that has been addressed qualitatively.

There are two important areas in which we expect this procedure to prove useful. One is an extremely large statistical study of FACs, as we demonstrated for the nightside R1 current. A statistical comparison of FAC signatures with other measurements such as particle precipitation is one of the most reasonable applications. The other area is the real-time monitor of the space environment. The procedure works at a reasonable speed even on an ordinary PC platform. Thus, it is possible to determine and announce the location and intensity of FACs as soon as data are transmitted to the ground. An automatic procedure such as reported in this paper could change the way we study FACs in the future.

Acknowledgments. The DMSP-F7 magnetometer data were provided by F. J. Rich. Work at JHU/APL was supported by NASA, NSF, and the Office of Naval Research. Work at the Institute of Statistical Mathematics was in part carried out under the ISM cooperative Research Program (H9-ISM.CRP-B7 and H10-ISM.CRP-B12).

REFERENCES

Akaike, H., A new look at the statistical model identification, *IEEE Trans. Autom. Control, AC 19*, 716, 1974.

Cummings, W. D., and A. J. Dessler, Field-aligned currents in the magnetosphere, *J. Geophys. Res., 72*, 1007, 1967.

Feldstein, Y. I., and G. V. Starkov, Dynamics of auroral and polar geomagnetic disturbances, *Planet. Space. Sci., 15*, 209, 1967.

Higuchi, T., Frequency domain characteristics of linear operator to decompose a time series into multi-components, *Ann. Inst. Stat. Math., 43*, 469, 1991.

Hiragi, Y., Urakawa, H., and Tanabe, K., Statistical procedure for deconvoluting experimental data, *J. Appl. Phys., 58*, 5, 1985.

Iijima, T., and T. A. Potemra, Field-aligned currents in the dayside cusp observed by Triad, *J. Geophys. Res., 81*, 5971, 1976.

Kamide, Y., and S.-I. Akasofu, Latitudinal cross section of the auroral electrojet and its relation to the Interplanetary magnetic field polarity, *J. Geophys. Res., 79*, 3755, 1974.

Kitagawa, G., and T. Higuchi, Automatic transaction of signal via statistical modeling, *Proc. First Int. Conf. Discovery Sci.*, Springer-Verlag Lecture Notes in Artificial Intelligence Series, *1532*, 375, 1998.

Richmond, A. D., and Y. Kamide, Mapping electrodynamic features of the high-latitude ionosphere from localized observations, Technique, *J. Geophys. Res., 93*, 5741–5759, 1988.

Sakamoto, Y., M. Ishiguro, and G. Kitagawa, *Akaike Information Criterion Statistics: Mathematics and its Application*, Boston, D. Reidel, 1986.

Weimer, D. R., A new technique for the mapping of ionospheric field-aligned currents from satellite magnetic field data, in this issue, 1999.

Zmuda, A. J., J. H. Martin, and F. T. Heuring, Transverse magnetic disturbances at 1100 km in the auroral region, *J. Geophys. Res., 71*, 5033, 1966.

T. Higuchi, The Institute of Statistical Mathematics, Tokyo 106, Japan.

S. Ohtani, The Johns Hopkins University Applied Physics Laboratory, 11100 Johns Hopkins Road, Laurel, MD, 20723-6099, U.S.A.